Vehicles Selection Algorithm for Cooperative Localization Based on Stochastic Geometry in Internet of Vehicle Systems

Wengang Li, Mohan Liu, Tianfang Chen, Guoqiang Mao

***Abstract*—In the face of the high density of vehicle distribution in urban areas, the self-organized network formed between vehicles has suffered serious communication interference, which will lead to the interruption of communication between vehicles and the inability of collaborative positioning. However, this issue has received little attention, and traditional cooperative positioning methods are no longer suitable for the network of high-density vehicles. In order to solve the cooperative localization issue in high-density vehicle networks, This paper proposes a region-constrained vehicle cooperative localization algorithm based on stochastic geometry. By setting restricted areas of vehicles, the communication capability and network capacity between vehicles are effectively improved. Then, to take full advantage of the density of the Ultra-high density vehicles network, the Geometric Dilution of Precision (GDoP) metric is used to dynamically introduce cooperative vehicles. By dynamically selecting vehicles, the value of GDoP decreases significantly with the increase of vehicle density. Finally, experimental simulations show that the network capacity in the vehicle system is improved by about 71% at the maximum interruption probability when using vehicle selection with restricted areas. Furthermore, the positioning performance of vehicles improves continuously with the increasing density of the cooperative vehicle network.**

***Index Terms*—Geometry dilution of precision(GDoP), Stochastic geometry, Signal to interference and noise ratio, System Capacity, Vehicle selection**

I. Introduction

With the advent of 5G era, Internet of Vehicles technology has been flourishing. The Internet of Vehicles takes vehicles in motion as information sensing objects, realizing network connection with surrounding objects through wireless communication technology. Among them, high-precision positioning technology is one of the key technologies of Internet of Vehicles. In order to improve the positioning accuracy of vehicles, many researchers have proposed multi-sensor-based fusion localization techniques [1-3], where IoT sensor devices are installed in each vehicle. However, the integration of multiple sensors in vehicles leads to an increase in the cost and power consumption of Internet of Vehicles. Unlike multi-sensor fusion localization techniques, collaborative vehicle localization [4-9] uses only the connectivity information of the vehicles in the network to achieve localization, avoiding the integration of multiple sensors in the vehicle. Current collaborative vehicle positioning generally relies on GPS navigation systems, but in urban areas, satellite signals loss is a challenging issue due to the effects of tall and dense buildings [10-13]. In addition, the expensive satellite receivers of vehicle terminals are not suitable for network of high density vehicles. Therefore, Vehicle-to-vehicle communication(V2V)-based cooperative vehicle localization methods are crucial. In V2V cooperative vehicle localization, these systems achieve precise positioning through inter-vehicle ranging information. However, when multiple vehicles are present in a certain area, choosing which vehicles to communicate with will affect the resulting positioning accuracy. Therefore, vehicle selection is crucial. The vehicle location information obtained by ranging techniques depends heavily on the vehicle topology, it is crucial to make a suitable vehicle selection. Therefore, this paper focuses on the vehicle selection strategy.

In cooperative localization, node selection has attracted the interest of many researchers. Most current node selection algorithms utilize fixed anchor nodes as auxiliary nodes for collaborative localization. However, the positioning performance of the system varies with the selection of anchor nodes. In wireless networks, the node selection algorithm based on path loss factor [14] calculates the path factor of signal transmission using the RSSI data measured in the system to obtain the point with the minimum path loss factor. However, the RSSI approach is susceptible to complex environments and multipath effects, especially in urban areas. The distance-based node selection algorithm uses the RSSI data measured in the system to calculate the test distance between the target node and the neighboring nodes and selects the neighboring nodes that are closer to the target node as auxiliary nodes. This method is also not applicable in urban environments due to the limitations of the RSSI method. The node selection algorithm, based on EFIM [15-16], initially computes the Fisher Information Matrix (FIM) for nodes using the signal model. It then decomposes and quantizes the FIM to derive EFIM, introduces SPEB to assess positioning accuracy, and ultimately chooses N nodes with the smallest SPEB as auxiliary nodes. However, the algorithm involves a large number of matrix operations, making it unsuitable for scenarios with a large number of nodes. The energy-based node selection algorithm [17-18] determines the communication radius of a node based on the energy of the system and selects the nodes within the communication range of the target node as auxiliary nodes. However, this method can only communicate within a fixed range of a node and cannot benefit the presence of high-density dynamic vehicles in the city. The distributed RSSI-based node selection algorithm [19] selects nodes with larger RSSI data as

This research is supported by NSFC grant, Grant number: U21A20446 (Corresponding author:Mohan Liu)

auxiliary nodes in the entire network, based on the RSSI data received by the sensor nodes. However, it still cannot address the scenario of high-density vehicle distribution in urban areas.

In addition to the above algorithms, there are also algorithms that study the geometric deployment of anchor nodes. By deploying anchor nodes in different regions, the unknown nodes in the region can be located more accurately. Therefore, it is necessary to systematically study the impact of anchor node deployment mode on positioning performance. Some researchers have also proposed many anchor node deployment schemes based on optimal positioning performance. Literature[20] proposes to deploy the anchors where the MSE lower bound is minimized to minimize the MSE. And [21] propose an optimization based method for joint anchor deployment and power allocation to achieve high-precision localization in wireless networks. In order to optimize the deployment of anchor nodes and make the estimation accuracy of positioning parameters more accurate, [22] formulates the optimal anchor placement problem in the form of the Fisher information matrix combination. Besides, due to geographical constraints, communication problems between sensors, and security issues, nodes cannot be simply placed in any position. In the literature [23], a method is proposed based on an optimality criterion to determine the optimal sensor-target geometry considering distance localization while accounting for sensor location constraints. However, in certain specific environments, nodes are dynamically randomized and cannot be deployed as anchor nodes in advance. Therefore, positioning methods based on distance distribution are widely proposed. Literature [24-25] proposes a scheme called Relative Urban Positioning System (RUPS) to address the relative distance fixing problem. Determining the positions of urban vehicles using GSM-aware trajectories has achieved good temporary stability, geographic uniqueness, and fine resolution. Literature [26] proposes an online distributed neighbor distribution estimation scheme, which effectively captures the distribution of surrounding vehicles and supports a more adaptive Media Access Control (MAC) protocol. Literature [27] proposes a node selection algorithm based on the location accuracy factor. This algorithm uses the contribution value of nodes with a contribution GDOP value greater than the threshold as the evaluation criteria for the overall network, and selects them as auxiliary nodes. By using GDoP as the evaluation standard of positioning performance criteria for positioning performance can avoid the need to deploy anchor nodes in advance. However, in the context of a 5G-based mobile vehicular self-organizing network, there will be a large number of vehicular nodes connecting to the network. Combining the aforementioned works, there are currently few dynamic and stochastic methods adapted for high-density scenarios in VANETs.In the future 5G-enabled V2V communication networks, the high density distribution of vehicles can easily lead the system into a state known as interference-limited mechanism. This results in increased interruption probabilities, reduced capacity for accommodating nodes in the network, blocked communication links, and decreased precision in collaborative positioning. On one hand, VANETs are a type of wireless network established in the field of vehicular networking based on Mobile Ad-Hoc Network (MANET), which inherently operates in an interference-limited environment, where interference escalates with the increase in network node density. On the other hand, the development of 5G networks not only increases network capacity by over a hundredfold but also promotes the densification of vehicles. Consequently, addressing the key challenge of enhancing the positioning accuracy and continuity of vehicles in vehicular networks through V2V cooperative positioning in high-density, high-interference networks, and leveraging the advantages of densification in 5G networks is imperative in the face of future trends towards high-density networks. So far as we all know, no works have focused on the effect of density and interference.

This paper is interested to the research of vehicle collaborative location in high-density vehicle scenarios and attempts to solve the interference between vehicles. In this paper, we propose a cooperative vehicle selection algorithm for Ultra-high density vehicles distribution. We model the stochastic geometry of the Ultra-high- density vehicles in the city and reduce the interference between vehicles by using the area restriction mechanism, and then use GDoP as the evaluation criterion for the cooperative vehicle selection.

In this paper, we primarily encounter three challenges. First, when analyzing cooperative strategies for vehicles, it is necessary to model the vehicles. However, with the support of 5G technology, the network structure of the Internet of Vehicles (IoV) becomes more heterogeneous and densely populated, increasing the complexity and irregularity of network topology. In this context, traditional modeling methods appear too idealized and are difficult to adapt to the practical needs of future IoV in terms of dynamics and density. Stochastic geometry, as a mathematical tool for analyzing wireless networks and modeling, can be used to capture the spatial random distribution of vehicles on the road as their density changes. To better align with real-world scenarios, nodes can be abstracted as corresponding spatial point processes. Compared to traditional geographic modeling methods, spatial point processes are more suitable for illustrating the node distribution in self-organizing vehicle networks, which is crucial for studying vehicle selection methods in VANETs.

Second, for channel modeling between vehicles, it is necessary to consider not only the channel conditions in real urban environments but also the complexity that the model brings to theoretical analysis. Therefore, we have studied a channel model for vehicle-to-vehicle communication that combines a large-scale path loss model and a small-scale propagation model. Additionally, considering that the focus of the paper is primarily on deriving the interference between vehicles—interference that is mainly influenced by vehicle distribution, power attenuation, and small-scale fading—we simplify the model by neglecting other factors with lesser impact, concentrating mainly on the power attenuation factor. In future applications, we will explore how to more comprehensively incorporate other factors into the model to enhance its accuracy and applicability.

Third, When analyzing the capacity of vehicular networks, it is necessary to study the communication interruption probability between vehicles. However, in mathematical terms, the

generalized integral for interruption probability does not yield a closed-form solution. Therefore, we consider studying the upper and lower bounds of the interruption probability. By combining these with stochastic geometry tools, we derive the network capacity, providing a foundation for subsequent analysis.

The main contribution of the paper is to propose selecting as many vehicles as possible to assist in positioning in the 5G ultra-dense vehicle network. The method is significant effective in reducing GDOP and improving vehicle positioning performance, and can give full play to the advantages of the densification of the 5G ultra-dense network. The rest of this paper is organized as follows: In Section II, we describe the system model. Section III describes the proposed algorithm in detail. Section IV describes simulation results and analysis. Finally, Section V concludes this paper.

II. System Model

In this section, to better present the algorithm, the system model in this paper is as follows

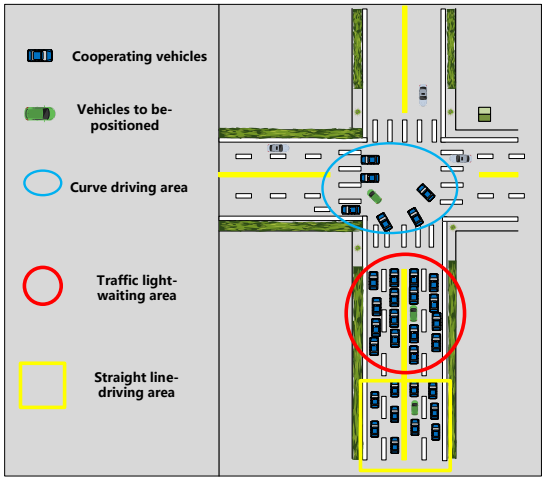

Fig. 1. Typical mega-vehicle distribution scenarios in cities.

A. Scenario of Vehicles

This paper presents a study of vehicle positioning in urban road networks, using four streets as an example. We establish three distinct vehicle driving areas: straight-line driving, traffic light waiting, and curved driving. As depicted in Fig. 1, the traffic density is highest in the traffic light waiting area and lowest in the curved driving area. Based on prior knowledge of vehicle traffic volume, we assume three different density distributions as $\lambda = \lambda_1, \lambda_2, \lambda_3$. We assume that each vehicle is equipped with distance measuring devices and can communicate wirelessly with other vehicles in the network. The assisting vehicles in our study are referred to as cooperative vehicles.

In our proposed approach, the vehicles in the city are modeled as a dynamic Poisson Point Process(PPP), and the angle θ between the vehicles to be positioned and the Cooperative vehicles is a random variable dependent on the vehicle density λ, as detailed in Part III of this paper. The vehicles to be positioned are located within a circle centered on the cooperative vehicles, with a communication radius of R, as illustrated in Figure 2.

Fig. 2. Diagram of the relative position of the cooperative vehicle and the vehicle to be positioned

B. Internet of Vehicle Communication Channel Model

The wireless channel model forms the foundation of communication system design and optimization, network deployment, and planning. The accurate modeling of the channel through simulation and research is crucial for providing a valuable basis for the deployment and implementation of actual networks. This paper presents a channel model for V2V communication, which combines a large-scale path loss model with a small-scale propagation model. When considering only large-scale fading, the signal energy of the transmitted signal per unit energy is reduced to R^{-k} after propagating a distance R. By defining the small-scale power fading factor as H, the channel fading model between vehicles can be expressed as follows:

$$g(d) = HR^{-k} \tag{1}$$

where k is the path attenuation coefficient.

We define H_{ij} as the power fading factor between the cooperative vehicle and the vehicle to be positioned. The cooperativeg vehicle and the vehicle to be positioned which are currently communicating, are denoted as T0 and R0, respectively. Except for the signal sent by R0, all signals received from the cooperative vehicle at T0 are considered as interference signals. Defining the transmitting power of the cooperative vehicle as P_i, the total interfering signal power received out at R0 can be expressed as

$$\Gamma_N = \sum_{i \in N} P_i H_{T_i R} R_{T_i R}^{-k} \tag{2}$$

We define θ as the minimum threshold to ensure normal communication between vehicles, and the probability of interruption at R0 can be calculated from Equation (3) as follows:

$$I(\lambda) = P(SINR < \theta) \tag{3}$$

Where $SINR$ is expressed as

$$SINR = \frac{PH_{T_0R}R_{T_0R}^{-k}}{\sum\limits_{i\in N} P_i H_{T_iR} R_{T_iR}^{-k}} \tag{4}$$

Where P is the signal power of the cooperative vehicles accessed to the positioning system in the current time slot.

Therefore, the mathematical expression of the disruption probability ignoring the effect of thermal noise is

$$I(\lambda) = P((SIR < \theta)|R_g) \tag{5}$$

where R_g is the distance and orientation between the vehicle to be positioned and other cooperative vehicles at a certain vehicle distribution density. From the outage probability $I(\lambda)$, we can obtain the communication capacity at T0 later.

III. Vehicle Selection Scheme for Cooperative Vehicles in Very High Density of Vehicle Scenario

In this section, we employ stochastic geometry to model the high-density distribution of vehicles and investigate the selection scheme of cooperative vehicles based on the difference in vehicle distribution density in various scenarios. The objective is to leverage the vehicle node selection scheme and take advantage of the densification of the ultra-dense vehicle network.

A. Stochastic Geometry Vehicle Modeling

We propose a novel approach based on stochastic geometry to analyze vehicle selection in localization systems for ultra-high-density vehicle populations. To capture the spatial random distribution of vehicles in urban roads with density variations, we use a stochastic geometric model and build different vehicle distribution densities to analyze the system. Our main idea is to represent the spatial locations of vehicles in urban lanes as corresponding point processes. Among these stochastic point processes, the most important and simple one is the Homogeneous Poisson Point Process (HPPP).

In this paper, assuming that the distribution of K vehicles in the entire vehicular network follows HPPP with parameter λ, and the vehicles are mutually independent. The distribution function $\prod(A)$ of the number of vehicles in any bounded region A is as follows:

$$P(\Pi(A) = k) = \exp(-\lambda A)\frac{(\lambda A)^k}{k!} \tag{6}$$

where λA is Lebesgue Measure[28], and A is a bounded region.

Later in this paper, we conduct multiple simulations of the planar HPPP to evaluate the performance of the selection scheme for cooperative vehicles. We analyze the statistical and analytical results of these simulations, and the final results represent the average performance that the selection scheme should have in the entire planar network.

B. Vehicle Collaboration Strategy Based on Restricted Areas

In a 5G-based ultra-dense V2V self-organizing mobile network, any vehicle can communicate wirelessly with any other vehicle in the network. All vehicles initiate communication with a certain probability in any time slot and communicate on the same communication frequency band. However, at high vehicle densities, communication between vehicles can interfere with each other, which impacts system capacity. The system capacity [30] is defined as the number of vehicles that can successfully communicate in a unit area network under the maximum interruption probability. To solve this problem, we propose a region-restricted vehicle communication strategy.

Within a time slot, cooperative vehicles T initiate communication with the vehicle R to be positioned based on their respective time slots. Only one vehicle communication pair exists in this time slot, and communication initiated by other vehicles will cause interference. The interference generated by cooperative vehicles depends mainly on the distance from R; cooperative vehicles closer to R will cause greater interference, which will result in lower SINR at R. In this paper, we introduce a restricted region at R, where vehicles within this region stop transmitting data. However, setting the restricted region too large reduces the density of cooperative vehicles at the transmitting node, which lowers the number of cooperative vehicles and increases the Geometric Dilution of Precision (GDoP). Conversely, setting the restricted region too small will cause excessive interference, which affects communication between vehicles. Therefore, this paper proposes an optimal restriction zone.

To obtain the optimal restricted area, it is necessary to derive the system capacity, and the prerequisite for deriving the system capacity is to calculate the interruption probability. According to the model in Section II ,the expression for interruption probability is:

$$I(\lambda) = P(\frac{H_{T_0R}{R_{T_0R}}^{-k}}{\Sigma_{i\in N} H_{T_iR}{R_{T_iR}}^{-k}} < \theta) \tag{7}$$

Where H_{T_iR} is the power fading coefficient between Ti and R, R_{T_iR} is the distance between Ti and R, and k is the path fading coefficient. When the SINR at the receiver R falls below the threshold θ, the communication will be interrupted. And then, we will transform equation (7) to obtain the following formula

$$P(H_{T_0R} < \theta {R_{T_0R}}^{-k} \Gamma_N) \tag{8}$$

Where

$$\Gamma_N = \Sigma_{i\in N} H_{T_iR}{R_{T_iR}}^{-k} \tag{9}$$

Using the distribution function of the first part H_{T_iR}, Equation (7) can be expressed as follows:

$$\begin{aligned} I(\lambda) &= E\left[\int_0^{\theta R_{T_0R} R_{R-\Gamma_N}} \mu \exp(-\mu x) dx\right] \\ &= 1 - E\left[\exp\left(-\mu\theta R_{T_0R}^{-k}\Gamma_N\right)\right] \\ &= 1 - L_{\Gamma_N}\left(\mu\theta R_{T_0R}^{-k}\right) \end{aligned} \tag{10}$$

where $L_{\Gamma_N}(\bullet)$ is represents the Laplace transform of the probability density function of the total interfering signal. Additionally, as the radius of the restricted area region set at R is d, Equation (10) can be expressed as follows:

$$I(\lambda) = 1 - \exp(-2\pi\lambda \int_d^\infty \frac{sx^{-k+1}}{sx^{-k}+c}) \tag{11}$$

Bringing equation (11) into equation (10) yields the expression as

$$I(\lambda) = 1 - \exp(-2\pi\lambda \int_d^\infty \frac{x^{-k+1}}{x^{-k}+\theta^{-1}R^{-k}}) \tag{12}$$

As Equation (12) contains generalized integrals, it is not feasible to perform calculations and obtain specific expressions for the interruption probability. Therefore, we analyze the upper and lower bounds of the interruption probability. From Equation (12), we can derive the upper bound of the interruption probability as follows:

$$\begin{aligned} I(\lambda) &= 1 - \exp(-2\pi\lambda \int_d^\infty \tfrac{x^{-k+1}}{x^{-k}+\theta^{-1}R^{-k}}) \\ &\le 1 - \exp(-2\pi\lambda \int_0^\infty \tfrac{x^{-k+1}}{x^{-k}+\theta^{-1}R^{-k}}) \\ &\le 1 - \exp[-\tfrac{2}{k}\lambda\pi^2 R^2 \theta^{\frac{2}{k}} \csc(\tfrac{2}{k}\pi)] \end{aligned} \tag{13}$$

Next, to derive the lower bound for the interruption probability, we resort to the concept of coverage probability. The expression for the coverage probability is $C_{ov}(\lambda) = P(SINR > \theta)$. Then, the interruption probability can be written as

$$\begin{aligned} I(\lambda) &= 1 - P(SINR > \theta) \\ &= 1 - P\left(\frac{H_{T_0R}R_{T_0R}^{-k}}{\sum_{i\in N} H_{T_iR}R_{T_iR}^{-k}} > \theta\right) \\ &> 1 - P\left(\frac{H_{T_0R}R_{T_0R}^{-k}}{H_{T_iR}R_{T_iR}^{-k}} > \theta\right) \\ &= 1 - P\left(d < R_{T_iR} \mid < \theta^k {H_{T_iR}}^k {H_{T_0R}}^{-k} R_{T_0R}\right) \end{aligned} \tag{14}$$

As shown in Equation (14), the lower bound of the interruption probability represents the probability of any coordinated vehicle falling into the main interference area. Thus, the interruption probability can be expressed as follows:

$$I(\lambda) = 1 - \exp(-\lambda S) \tag{15}$$

where S represents the area of the main interference area. Let $\frac{H_{T_iR}}{H_{T_0R}} = h$ and according to its Probability Density Function(PDF) formula for the power attenuation factor, we can be obtained the probability density function of h as $f_H(h) = \frac{1}{(1+h)^2}$, and from equation (14) can be obtained $H > \theta^{-1}R_{T_0R}^{-k}d^k$, then the expression of the area of the main interference area S as

$$\begin{aligned} S &= \int_{\theta^{-1}R_{T_0R}^{-k}d^k}^\infty \frac{1}{(1+h)^2} \int_d^{h^{\frac{1}{k}}\theta^{\frac{1}{k}}R_{T_0R}} 2\pi x dx dh \\ &= \pi\theta^{\frac{2}{k}} R_{T_0R}^2 [\frac{1}{k-2} + \ln(\frac{2}{1+d^2R_{T_0R}^2\theta^{-\frac{2}{k}}})] \end{aligned} \tag{16}$$

So the expression for the lower bound of the corresponding interruption probability as

$$I(\lambda) = 1 - \exp\{-\lambda\pi\theta^{\frac{2}{k}} R_{T_0R}^2 [\frac{1}{k-2} + \ln(\frac{2}{1+d^2R_{T_0R}^2\theta^{-\frac{2}{k}}})]\} \tag{17}$$

In summary, the upper and lower bounds of the interruption probability show that the interruption probability increases with the increase of the density of vehicles, i.e., the interference between vehicles will be large in the ultra-dense vehicle environment.

To solve this problem, the optimal restricted area radius d is derived next, and solving for $I(\lambda) = P_{\max}$ according to equation (12), we can get

$$\lambda_T = \frac{-\ln(1-P_{\max})}{2\pi \int_d^\infty \frac{x^{-k+1}}{x^{-k}+\theta^{-1}R_{T_0R}^{-k}}} \tag{18}$$

In the entire urban vehicular network, the distribution density of all vehicles is denoted as λ. At any given time slot, a vehicle sends data with probability P. Therefore, the density of cooperative vehicles is λP. Due to the existence of the restricted area, the final density of cooperative vehicles can be expressed as:

$$\lambda_T = \lambda p \exp(-\lambda_T p \pi d^2) \tag{19}$$

let $\frac{\partial\lambda_T}{\partial\lambda} = 0$ and solve it, and bring it into Eq. (19) to obtain $\lambda_T \le \frac{1}{\pi e d^2}$, so that Eq. (18) equals $\frac{1}{\pi e d^2}$, and finally obtain the optimal restricted area radius as

$$d = \sqrt{\frac{\frac{2}{k}\theta^{\frac{2}{k}} R^2 \pi \csc\left(\frac{2}{k}\pi\right)}{1 - e\ln(1-P_{\max})}} \tag{20}$$

Based on the optimal restricted area radius obtained in the previous section, this section proposes a method to solve the selection of ultra-high density vehicles for cooperative localization. Firstly, we define three different vehicle distribution densities, denoted as $\lambda = \lambda_1, \lambda_2, \lambda_3$, based on the a prior information of three scenarios in the city. Accordingly, the GDoP threshold $g = g_1, g_2, g_3$, the maximum interruption probability $P\max = P_1, P_2, P_3$, and the signal-to-noise ratio threshold $\theta = \theta_1, \theta_2, \theta_3$ are designed. In addition, due to the ranging devices of the vehicles, each vehicle obtains the distance information $R = R_1, R_2, ..., R_N$ of all vehicles within the communication range before communication is carried out. Next, two thresholds, denoted as $\beta = \beta_1, \beta_2$, are set, and based on the relationship between N and β, the corresponding scenario is selected. Finally, by inputting $P_{\max}, \theta, R$, we can obtain $d_1, d_2, ..., d_N$, and the number of vehicles within the radius of d that are allowed to communicate with the vehicle to be positioned is restricted. Assuming that the vehicle that successfully communicates is denoted as $S = S_1, S_2, ..., S_M$, the angle $\alpha = \alpha_1, \alpha_2, ..., \alpha_M$ from the communicating vehicle to the vehicle to be positioned can be measured, and α is then incorporated into equation (34) to calculate the GDoP of this vehicle selection scheme until the GDoP threshold is satisfied. The pseudocode of the algorithm is as follows:

Algorithm 1 Vehicle selection algorithm.

1: for each vehicle nodes to be located **do**

2: Obtain the estimated distance to the surrounding vehicle nodes $R_1, R_2, ..., R_N$

3: If N is less than β_1, determine the scene density as λ_1

4: else if N is greater than β_1 and less than β_2, determine the scene density as λ_2

5: else determine the scene density as λ_3

6: Calculate N restricted areas:$d = \sqrt{\frac{\frac{2}{k}\theta^{\frac{2}{k}} R^2 \pi \csc\left(\frac{2}{k}\pi\right)}{1-e\ln(1-P_{\max})}}$ get $d = d_1, d_2, ..., d_N$

7: Get the vehicle with successful communication $S_1, S_2, ..., S_M$

8: Measure the angle information with M vehicles $\alpha_1, \alpha_2, ..., \alpha_M$

9: Bring into GDoP formula for calculation: $\sqrt{Trace[\bar{I}^{-1}(x)]}$, get $g^{'}$

10: if $g^{'}$ does not meet the set threshold ,go to step 14

11: else go to step 1

12: end if

13: end if

14: Increase the GDoP threshold accordingly,go to step 1

15: end for

IV. Simulation and Analysis

In this section, we perform a series of numerical simulations to demonstrate the effectiveness of the proposed vehicle selection scheme. In the first part, we adopt a logarithmic coordinate system in order to see the results more intuitively. Firstly, we perform a performance analysis of the relationship between the upper and lower bounds of the disruption probability and the vehicle density, and then we perform a performance analysis of the relationship between the network capacity and the maximum disruption probability with and without setting the restricted area. Finally, we perform performance analysis on the GDoP values of taking the number of fixed cooperative vehicles versus the number of dynamic cooperative vehicles under establishing different vehicle densities, respectively.

A. Simulation of Vehicle Communication Capacity Results Based on Restricted Areas

The communication distance R is set to 100 m, the SINR threshold θ is set to 3, and the path fading factor K is set to 4. As shown in the figure 3, both the upper and lower bounds of the probability of interruption increase with the increase in the density of vehicles, illustrating that in the Ultra-high density vehicles, interference between vehicle nodes will seriously affect communication between vehicles.

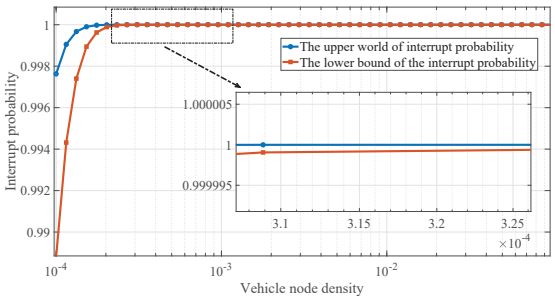

Fig. 3. Plot of interruption probability relative to co-vehicle density λ

In the following section, we analyze the effect of using the restricted area communication method on the interruption probability and compare the relationship between the network capacity and the interruption probability when using the restricted area and when not using it. When the limit of d approaches 0, the area of the restricted area in the network is 0. By substituting d=0 into equation (12), we obtain the expression for the interruption probability without the restricted area as follows:

$$I_{d=0}(\lambda) = 1 - \exp(-\frac{2}{k}\lambda\theta^{\frac{2}{k}} R^2\pi^2 \csc(\frac{2}{k}\pi)) \tag{21}$$

Let $I_{d=0}(\lambda) = P_{\max}$, we can obtain Tx of the cooperative vehicle with the maximum interruption probability as

$$\lambda = \frac{-\ln(1-P_{\max})}{\frac{2}{k}\theta^{\frac{2}{k}} R^2\pi^2} \sin(\frac{2}{k}\pi) \tag{22}$$

Then the expression of the network capacity without the restricted area as

$$C_{d=0} = \frac{-(1-P_{\max})\ln(1-P_{\max})}{\frac{2}{k}\theta^{\frac{2}{k}} R^2\pi^2}(\sin\frac{2}{k}\pi) \tag{23}$$

Remaining all other parameters unchanged, we calculate the optimal restriction area d to be 36.827m using formula (20). As shown in Figure 4, the network capacity with the presence of the optimal restricted area is greatly improved compared to the network capacity with the unrestricted area. A network composed of vehicles with ultra-high density is an interference-limited system, it is the overall interference intensity in the network that determines the number of vehicles available for collaboration in the network. After setting up restricted areas, interference around the vehicles to be positioned is reduced. Therefore, when considering the same maximum interruption probability, the network can accommodate a higher density of cooperative vehicles.

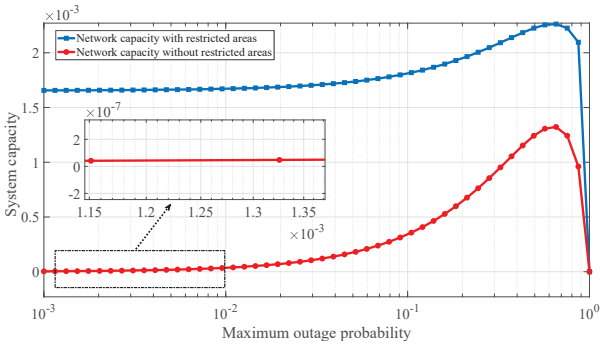

Fig. 4. Plot of transmission capacity versus maximum outage probability P_{max}

B. Calculation and Simulation Analysis of GDOP with Vehicles Density

The accuracy of the position depends on various factors, with the most important being distance precision and geometric factors. Therefore, in the absence of precise planning of the coverage area for cooperative vehicle positioning and quantity, GDoP may become the main factor affecting location accuracy. To analyze the variation of GDoP with urban vehicle density in two-dimensional space, an analytical model of GDoP is constructed in this paper. Moreover, the model was used to analyze the positioning performance of dynamic vehicle selection.

We set the coordinates of the vehicle to be precisely positioned to (x, y) , set the coordinates of all other vehicles used for coordination to (x_i, y_i) , and set the measured distance $\widehat{d}$ between the vehicle to be positioned and the other vehicles, denoted as

$$\widehat{d} = [\widehat{d_1}, \widehat{d_2}, ..., \widehat{d_N}] \tag{24}$$

For the vehicle to be positioned x, the conditional probability density function of $\widehat{d}$ can be expressed as

$$P(\hat{d}|x) = \prod_{i=1}^{N} \frac{1}{\sqrt{2\pi\sigma_i^2}} \exp\{-\frac{(\overset{\wedge}{d_i} - d_i)^2}{2\sigma^2}\} \tag{25}$$

According to the conditional probability density function provided in Equation (25), the Cramér-Rao Lower Bound (CRLB) can be obtained based on the location estimate mentioned above. Following Bayesian estimation theory, the covariance of the estimation error for any unbiased parameter estimate $\widehat{\alpha_i}$ must be constrained by a CRLB(α_i), which can be expressed as:

$$cov(\widehat{\alpha_i}) \geq CRLB(\alpha_i) \tag{26}$$

$$CRLB(\alpha_i) = J(\alpha_i)^{-1} \tag{27}$$

where $J(\alpha_i)^{-1}$ denotes the Fisher Information Matrix (FIM). And the localization accuracy information corresponding to the Bayesian estimation of the vehicle x can be fully inscribed by the FIM $J(\alpha_i)^{-1}$ of the full variable α_i, whose FIM is defined as

$$J(\alpha_i) = -E_{\alpha_i, z_i}\{\nabla_{\alpha_i, \alpha_i{}^T} \ln p(z_i|\alpha_i)\} \tag{28}$$

where $\nabla_{\alpha_i, \alpha_i{}^T}$ is the second order derivative with respect to the full variable α_i.

Based on the FIM defined above, let us calculate a lower bound on the Clamerow conditional probability density of $\widehat{d}$. The elements of this matrix are defined as follows:

$$[I(x)]_{ij} = -E[\frac{\partial^2 lnP(\widehat{d}|x)}{\partial x_i \partial x_j}] \tag{29}$$

Bringing equation (25) into equation (29) yields the expression for the FIM as

$$\begin{aligned} I(x) &= \begin{bmatrix} \sum_{i=1}^{N} \frac{(x-x_i)^2}{\sigma^2 d_i^2} & \sum_{i=1}^{N} \frac{(x-x_i)(y-y_i)}{\sigma^2 d_i^2} \\ \sum_{i=1}^{N} \frac{(x-x_i)(y-y_i)}{\sigma^2 d_i^2} & \sum_{i=1}^{N} \frac{(y-y_i)^2}{\sigma^2 d_i^2} \end{bmatrix} \\ &= \begin{bmatrix} \sum_{i=1}^{N} \frac{\cos^2(\alpha_i)}{\sigma^2} & \sum_{i=1}^{N} \frac{\cos(\alpha_i)\sin(\alpha_i)}{\sigma^2} \\ \sum_{i=1}^{N} \frac{\cos(\alpha_i)\sin(\alpha_i)}{\sigma^2} & \sum_{i=1}^{N} \frac{\sin^2(\alpha_i)}{\sigma^2} \end{bmatrix} \end{aligned} \tag{30}$$

α denotes the angle from the co-vehicle to the vehicle to be positioned, then the CRLB can be given by $I^{-1}(x)$. Based on the positioning for any estimate $\hat{x}$ of the vehicle position obtained using the unbiased estimator are

$$E_x[(\hat{x} - x)(\hat{x} - x)^T] \geq I^{-1}(x) \tag{31}$$

Since in this paper we mainly analyze the performance of CRLB for different vehicle selection schemes, the common factor σ^2 in equation (30) is extracted and simplified as

$$\overline{I} = \sigma^2 I \tag{32}$$

Where $\overline{I}$ can be expressed as

$$\bar{I}(x) = \begin{bmatrix} \sum_{i=1}^{N} \cos^2(\alpha_i) & \sum_{i=1}^{N} \cos(\alpha_i)\sin(\alpha_i) \\ \sum_{i=1}^{N} \cos(\alpha_i)\sin(\alpha_i) & \sum_{i=1}^{N} \sin^2(\alpha_i) \end{bmatrix} \tag{33}$$

Based on the above theory, we can conclude that in the scenario of a network of ultra-dense vehicles, $\alpha = \{\alpha_1, \alpha_2, ..., \alpha_N\}$ is sufficiently necessary for analyzing the localization performance, which will affect the CRLB of localization accuracy. The set of parameters $\alpha = \{\alpha_1, \alpha_2, ..., \alpha_N\}$ varies depending on the different options of synergistic vehicles. Thus, different schemes for selecting vehicles will have a direct impact on the Cramér-Rao lower bound (CRLB) of localization accuracy.

It is further simplified into GDOP according to Eqs. (27), (28) and (29) as

$$GDOP = \sqrt{Trace[(I^{-1}(x)]} \tag{34}$$

$$GDOP = \sqrt{CRLB} \tag{35}$$

$$GDOP = \sqrt{Trace[(\bar{I}^{-1}(x)]} \tag{36}$$

To summarize, when selecting vehicles for cooperative positioning, the difference in optimal positioning performance of

different vehicle selection schemes can be fully represented by the GDoP, regardless of whether the current distribution density of corresponding vehicles is the same.

The use of a restricted area vehicle communication strategy can significantly increase the number of vehicles in the network. Therefore, it is necessary to study the performance of cooperative localization schemes at different densities in the presence of ultra-high density vehicles. In traditional cooperative vehicle localization, a fixed number of vehicles are selected in a certain geometric pattern to collaborate with the vehicles to be positioned. In an ultra-high density vehicle network, if the number of selected collaborating vehicles is fixed according to the PPP, only the distance between the vehicle to be positioned and the cooperative vehicle needs to satisfy a certain probability distribution. The angle θ between the vehicle to be positioned and the cooperative vehicle is a random variable independent of density, and the cooperative vehicles are distributed in a circular pattern around the vehicle to be positioned.

Then in terms of the average GDoP, for fixed scenarios the expression exists as

$$E_\theta\{Tr(\bar{I}^{-1})|\lambda\} = E_\theta\{Tr(\bar{I}^{-1})\} \tag{37}$$

Equation (37) is validated below by simulating an ultra-high density vehicle network using a HPPP. For example, considering a vehicle to be positioned at the origin, the performance of the selection scheme in the entire network is obtained by analyzing the variability of different cooperative selection schemes at that vehicle. Monte Carlo experiments are used to average the results for each scheme at each distribution density. To reduce computational complexity, a scenario with four lanes in a 160 m × 25 m urban area is selected, with an initial vehicle distribution density of $40/(4000m^2)$. The data has been subjected to corresponding fitting processing for easy visualization. Figure 6 shows that the fitted line segments are close to straight lines for different values of N. The correlation fitting coefficients for $N = 4$ and $N = 7$ are $R_{N=4} = -0.0685$ and $R_{N=7} = -0.0605$, respectively, and the corresponding P values are $P_{N=4} = 0.3864$ and $P_{N=7} = 0.3878$, respectively. The simulation results fully support the assertion of Eq.(35), which states that the GDoP is completely independent of the density of cooperative vehicles for a fixed number of vehicles scenario. Therefore, the lower limit of the localization accuracy of Cramerow will no longer change, and further densification of the vehicle network will not provide additional benefits.

In addition, it can be observed from Figure 5 that the average GDoP decreases as the number of participating vehicles increases in the ultra-high density vehicle network. This implies that the localization accuracy can be effectively enhanced with an increase in the number of participating vehicles. This paper proposes a vehicle selection scheme for cooperative vehicle positioning in different urban scenarios, based on setting different GDoP thresholds according to varying distribution densities in the case of ultra-high density vehicles. The scheme selects cooperative vehicles by continuously introducing the number of vehicles successfully communicating in the system

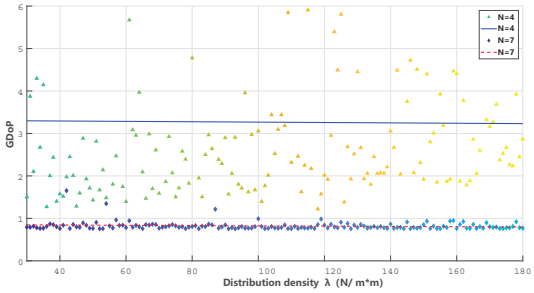

Fig. 5. Plot of simulation data of GDoP versus distribution density λ.

until the GDoP thresholds are met, as illustrated below. Figure 6 demonstrates the use of PPP to simulate vehicle distribution and provides the variation of GDoP for the scheme as the vehicle distribution density changes. The average GDoP at each density is obtained by taking the mean value of 500 Monte Carlo experiments. The correlation coefficient in Figure 6 is R=-0.59, with a P-value of 4.7×10^{-5}. Compared with Figure 5, the dynamic selection of cooperative vehicles for positioning can effectively improve GDoP, which indicates that the traditional selection of fixed vehicles for positioning does not fully utilize the advantages of dense networks. The optimal localization performance of the proposed scheme significantly benefits from the continuous densification of the ultra-high density vehicle network, unlike conventional schemes. The proposed scheme selects more vehicles when the vehicle density increases, and the relationship between GDoP and vehicle density is typically negative at this time. Therefore, the proposed scheme can effectively improve the CRLB of localization accuracy.

C. Simulation Analysis of Positioning Performance with Vehicle Density

To further illustrate the superiority of the localization performance of this algorithm in the 5G ultra-dense vehicle network, we experimentally analyze the localization error of the vehicles to be positioned for the selected fixed number of cooperative vehicles and the dynamic number of cooperative vehicles, respectively. Experimental results are shown in Figures 7 and 8. In Figure 8, the P-value of the fitted curve is 2.6×10^{-60}, and the correlation coefficient is R=-0.9133. Figure 7 further confirms the findings of Figure 5, as vehicle density increases and a fixed number of cooperative vehicles are selected for

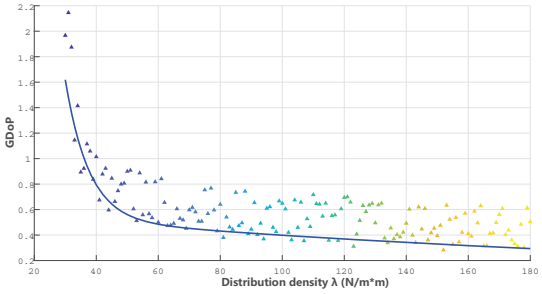

Fig. 6. Plot of GDoP versus distribution density λ under dynamic nodes

auxiliary positioning, the positioning accuracy of vehicles to be positioned does not improve, and the localization RMSE values remain unchanged. However, Figure 8 illustrates the results of dynamic selection of cooperative vehicles for positioning, indicating that the positioning accuracy of the vehicles to be positioned significantly improves with increasing vehicle density. Therefore, the best performance of localization is independent of the vehicle distribution density when a fixed number of cooperative vehicles are selected, and does not benefit from further densification of the vehicle network. On the other hand, when dynamically selecting cooperative vehicles, the localization RMSE value of the vehicles to be positioned decreases, indicating that selecting more vehicles for collaboration is necessary when the density of cooperative vehicles increases.

In summary, the proposed vehicle selection scheme is better suited for 5G ultra-dense vehicle networks than traditional methods, and has the potential to further improve localization performance as the vehicle communication network densifies in the future.

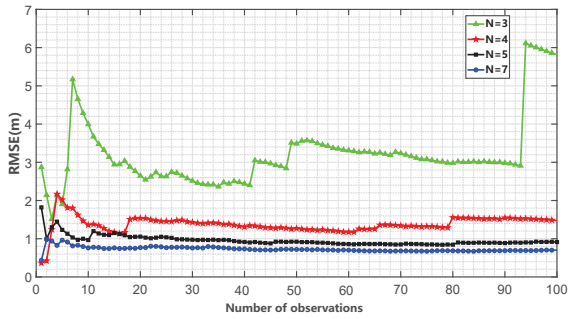

Fig. 7. Positioning performance of vehicles under different cooperative vehicles

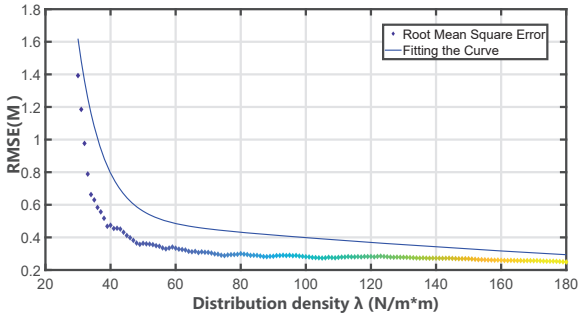

Fig. 8. Relationship between vehicle positioning performance and cooperative vehicle density

D. The existing algorithms comparison

We compare the proposed scheme with the method by Mukhopadhyay[27]. In order to adapt their technique to the problem consider in this work, we considered their second network protocol, placing their anchor nodes at random positions. We allowed all nodes in the network to move randomly, assuming that the positions of anchor nodes are known and setting all target nodes to have the same ranging range. In the digital simulation, we configured a constrained interference function that impacts the network capacity in a mobile ad-hoc network. We simulated both algorithms in this specific environment, and the simulation results are presented in Figure 9.

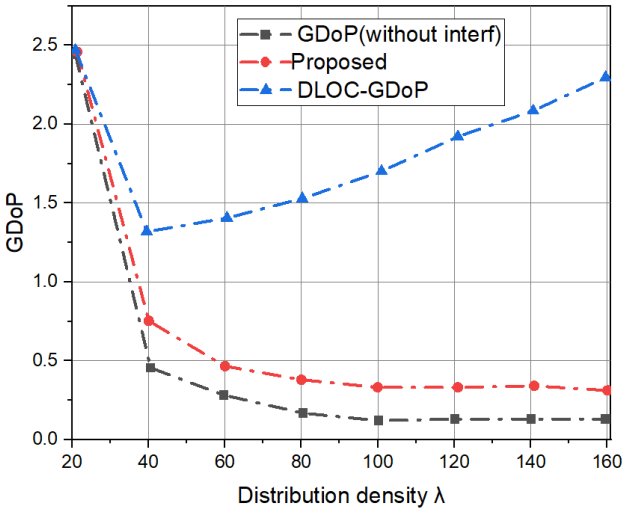

Fig. 9. Relationship between vehicle positioning performance and cooperative vehicle density

As shown in Figure 9, we compared GDoP without interference, our algorithm under interference, and the DLOC-GDoP algorithm. In the presence of communication interference between vehicles, the DLOC-GDoP algorithm is significantly constrained as vehicle density increases.

V. Conclusion

In this paper, we propose a cooperative vehicle selection algorithm based on stochastic geometry and restricted areas for ultra-high density vehicle networks. The ultra-high density vehicles in the city are modeled using a stochastic geometry approach, and the theory is analyzed using related tools. The proposed algorithm selects vehicles based on the restricted area to reduce interference between vehicles in the distribution of ultra-dense vehicles in the city, aiming to increase the network capacity of the entire vehicle network and improve the distribution density of cooperative vehicles in ultra-high density vehicle networks. We set different GDoP thresholds for a priori information of vehicle volume distribution density in three scenarios in the city and adaptively select cooperative vehicles according to the thresholds. Simulation results demonstrate that the algorithm can improve the network capacity by 71% at high vehicle distribution density and fully leverage the 5G ultra-dense vehicle network densification to enhance vehicle localization performance.

Appendix

Derivation of $L(\bullet)$

Let us review formula (10), in which we will use stochastic geometry tools to compute the Laplace transform.

$$\begin{aligned} I(\lambda) &= E[\textstyle\int_0^{\theta R_{T_0R}^{-k}\Gamma_N} \mu\exp(-\mu x)dx] \\ &= 1 - E[\exp(-\mu\theta R_{T_0R}^{-k}\Gamma_N)] \\ &= 1 - L_{\Gamma_N}(\mu\theta R_{T_0R}^{-k}) \end{aligned} \tag{38}$$

where $L_\bullet$ is the Laplace transform of the probability density function of the total interference signal

$$L_{\Gamma_N}(\mu\theta R_{T_0R}^{-k}) = \exp(-2\pi\lambda\textstyle\int_d^\infty \frac{sx^{-k+1}}{sx^{-k}+c}) \tag{39}$$

where $s = \mu\theta R_{T_0R}^{-k}$

When the network coverage is a circular area with the vehicle to be positioned as the center of the circle and the distance from the center of the circle is greater than d and less than r, the derivation for $L_{\Gamma_N}(\mu\theta R_{T_0R}^{-k})$ is derived as follows

$$\begin{aligned} L_{\Gamma_N|N}(\mu\theta R_{T_0R}^{-k}) &= E\left[\exp(-\mu\theta R_{T_0R}^{-k}\sum_{i=1}^{N} H_{T_0R}R_{T_iR}^{-k})\right] \\ &= \prod_{i=1}^{N} E\left[\exp(\mu\theta R_{T_0R}^{-k}\sum_{i=1}^{N} H_{T_0R}R_{T_iR}^{-k})\right] \\ &= \left\{E[\exp(-\mu\theta R_{T_0R}^{-k}H_{T_0R}R_{T_iR}^{-k}))]\right\}^N \end{aligned} \tag{40}$$

Since the vehicles are geometrically randomly distributed, the probability density function of the distance between any cooperative vehicle and the vehicle to be positioned is

$$f_{R_{T_iR}}(x) = \frac{2x}{r^2 - d^2} \tag{41}$$

$$\begin{aligned} L_{\Gamma_N|N}(\mu\theta R_{T_0R}^{-k}) &= \left\{E[\exp(-\mu\theta R_{T_0R}^{-k}H_{T_0R}x^{-k}))]\right\}^N \\ &= \left\{\int_d^r \tfrac{2x}{r^2-d^2}[\exp(-\mu\theta R_{T_0R}^{-k}\sum_{i=1}^{N} H_{T_iR}x^{-k})]dx\right\}^N \end{aligned} \tag{42}$$

Bringing equation (39) to equation (38) yields the expression

$$\begin{aligned} L_{\Gamma_N|N}(\mu\theta R_{T_0R}^{-k}) &= \left\{E[\exp(-\mu\theta R_{T_0R}^{-k}H_{T_0R}x^{-k})]\right\}^N \\ &= \left\{\left[\int_d^r \tfrac{2x}{r^2-d^2}\left[\exp(-\mu\theta R_{T_0R}^{-k}\sum_{i=1}^{N} H_{T_iR}x^{-k})\right]\right\}^N \end{aligned} \tag{43}$$

Using equations (18) and (37), we can obtain $L_{\Gamma_N}(\mu\theta R_{T_0R}^{-k})$ as

$$\begin{aligned} &L_{\Gamma_N}(\mu\theta R_{T_0R}^{-k}) \\ &= \sum_{N=1}^{\infty}\tfrac{(\pi r^2\lambda)^N}{N!}\exp(-\pi r^2\lambda) \\ &\times\left\{\tfrac{1}{\pi(r^2-d^2)}\int_d^r 2\pi E\left[\exp(-\mu\theta R_{T_0R}^{-k}H_{T_0R}x^{-k}\right]xdx\right\}^N \\ &= \exp(\left[-\pi r^2\lambda\right])\sum_{N=1}^{\infty}\tfrac{\lambda^N}{N!}\tfrac{(r^2)^N}{(r^2-d^2)^N} \\ &\times\left(\int_d^r 2\pi E\left[\exp(-\mu\theta R_{T_0R}^{-k}H_{T_0R}x^{-k})\right]xdx\right)^N \\ &= \exp\left\{\left[-\pi r^2\lambda\right] + \right. \\ &\left.\tfrac{r^2\lambda}{r^2-d^2}\int_d^r 2\pi E\left[\exp(-\mu\theta R_{T_0R}^{-k}H_{T_0R}x^{-k})\right]xdx\right\} \\ &= \exp\left\{\tfrac{r^2\lambda}{r^2-d^2}2\pi\int_d^r x\left\{E\left[\exp(-\mu\theta R_{T_0R}^{-k}H_{T_0R}x^{-k})\right]-1\right\}dx\right\} \end{aligned} \tag{44}$$

When $A \to \infty$

$$\begin{aligned} &L_{\Gamma_N}(\mu\theta R_{T_0R}^{-k}) = \\ &\exp\left\{2\pi\lambda\int_d^\infty x\left\{E\left[\exp(-\mu\theta R_{T_0R}^{-k}H_{T_0R}x^{-k})\right]-1\right\}dx\right\} \end{aligned} \tag{45}$$

Because $f_H(h) = \mu\exp(-\mu h)$

$$\begin{aligned} &E\left[\exp(-\mu\theta R_{T_0R}^{-k}H_{T_0R}x^{-k})\right] \\ &= \int_0^\infty \mu\exp(-\mu h)\exp(-\mu\theta R_{T_0R}^{-k}H_{T_0R}hx^{-k})dh \\ &= \tfrac{\mu}{\mu\theta R_{T_0R}^{-k}x^{-k}+\mu} \\ &= \tfrac{\mu}{sx^{-k}+\mu} \end{aligned} \tag{46}$$

Substituting equation (44) into (43) yields the expression

$$L_{\Gamma_N}(s) = \exp\left(-2\pi\lambda\int_d^\infty \frac{sx^{-k+1}}{sx^{-k+1}+\mu}\right) \tag{47}$$

REFERENCES

[1] Z. Xia and S. Tang, "Robust self-localization system based on multi-sensor information fusion in city environments," 2019 International Conference on Information Technology and Computer Application (ITCA), 2019, pp.

[2] X. Tao et al., "A Multi-Sensor Fusion Positioning Strategy for Intelligent Vehicles Using Global Pose Graph Optimization," in IEEE Transactions on Vehicular Technology, vol. 71, no. 3, pp. 2614-2627, March 2022.

[3] P. Yang, D. Duan, C. Chen, X. Cheng and L. Yang, "Multi-Sensor Multi-Vehicle (MSMV) Localization and Mobility Tracking for Autonomous Driving," in IEEE Transactions on Vehicular Technology, vol. 69, no. 12, pp. 14355-14364, Dec. 2020.

[4] X. Kong, H. Gao, G. Shen, G. Duan and S. K. Das, "FedVCP: A Federated-Learning-Based Cooperative Positioning Scheme for Social Internet of Vehicles," in IEEE Transactions on Computational Social Systems, vol. 9, no. 1, pp. 197-206, Feb. 2022.

[5] X. Hou, L. Luo, W. Cai and B. Guo, "E2T-CVL: An Efficient and Error-Tolerant Approach for Collaborative Vehicle Localization," in IEEE Internet of Things Journal, vol. 9, no. 5, pp. 3481-3494, 1 March1, 2022.

[6] H. Wang, L. Wan, M. Dong, K. Ota and X. Wang, "Assistant Vehicle Localization Based on Three Collaborative Base Stations via SBL-Based Robust DOA Estimation," in IEEE Internet of Things Journal, vol. 6, no. 3, pp. 5766-5777, June 2019.

[7] K. Ansari, "Cooperative Position Prediction: Beyond Vehicle-to-Vehicle Relative Positioning," in IEEE Transactions on Intelligent Transportation Systems, vol. 21, no. 3, pp. 1121-1130, March 2020.

[8] J. Xiong, J. W. Cheong, Z. Xiong, A. G. Dempster, S. Tian and R. Wang, "Hybrid Cooperative Positioning for Vehicular Networks," in IEEE Transactions on Vehicular Technology, vol. 69, no. 1, pp. 714-727, Jan. 2020.

[9] S. Nam, D. Lee, J. Lee and S. Park, "CNVPS: Cooperative Neighboring Vehicle Positioning System Based on Vehicle-to-Vehicle Communication," in IEEE Access, vol. 7, pp. 16847-16857, 2019.

[10] C. -H. Ou, B. -Y. Wu and L. Cai, "GPS-free vehicular localization system using roadside units with directional antennas," in Journal of Communications and Networks, vol. 21, no. 1, pp. 12-24, Feb. 2019.

[11] R. Rabiee, X. Zhong, Y. Yan and W. P. Tay, "LaIF: A Lane-Level Self-Positioning Scheme for Vehicles in GNSS-Denied Environments," in IEEE Transactions on Intelligent Transportation Systems, vol. 20, no. 8, pp. 2944-2961, Aug. 2019.

[12] F. Wang et al., "Geometry-Based Cooperative Localization for Connected Vehicle Subject to Temporary Loss of GNSS Signals," in IEEE Sensors Journal, vol. 21, no. 20, pp. 23527-23536, 15 Oct.15, 2021.

[13] C. Zhuang, H. Zhao, S. Hu, W. Feng and R. Liu, "Cooperative Positioning for V2X Applications Using GNSS Carrier Phase and UWB Ranging," in IEEE Communications Letters, vol. 25, no. 6, pp. 1876-1880, June 2021.

[14] Y. -F. Huang et al., "Indoor Positioning with Reference Nodes Selection in Wireless Networks," 2018 International Symposium on Computer, Consumer and Control (IS3C), 2018, pp. 445-448.

[15] S. Tian and Z. Zhang, "A Node Selection Algorithm Based on Multi-Objective Optimization Under Position Floating," in IEEE Access, vol. 10, pp. 41863-41873, 2022.

[16] Zhou F, Wang G. "Node selection algorithm based on Fisher information"[J]. EURASIP Journal on Wireless Communication and Networking,2016,2016(1):249.

[17] B. Li, H. Li, R. Zhang and C. Wei, "An Energy-efficient Metric for Relay Selection in Large-Scale Multi-hop Wireless Networks," 2019 International Conference on Computing, Networking and Communications (ICNC), 2019, pp. 771-776.

[18] T. Rahman, X. Yao, G. Tao, H. Ning and Z. Zhou, "Efficient Edge Nodes Reconfiguration and Selection for the Internet of Things," in IEEE Sensors Journal, vol. 19, no. 12, pp. 4672-4679, 15 June15, 2019, doi: 10.1109/JSEN.2019.

[19] S. -Y. Huang and R. -B. Wu, "Positioning for Search and Rescue in GPS-Denied Area by Distributed WiFi RSS-based DoA Modules," in IEEE Access, 2022.

[20] F. Zhou, L. Fan, J. Tang and W. Chen, "Placement and Concise MSE Lower-Bound for UAV-Enabled Localization via RSS," in IEEE Transactions on Vehicular Technology, vol. 71, no. 2, pp. 2209-2213, Feb. 2022.

[21] Z. Ma, F. Liu, H. Qiao, S. Liu and X. Lv, "Joint Optimization of Anchor Deployment and Power Allocation in Wireless Network Localization," in IEEE Communications Letters, vol. 24, no. 5, pp. 1086-1089, May 2020.

[22] N. Saeed, T. Y. Al-Naffouri and M. -S. Alouini, "Outlier Detection and Optimal Anchor Placement for 3-D Underwater Optical Wireless Sensor Network Localization," in IEEE Transactions on Communications, vol. 67, no. 1, pp. 611-622, Jan. 2019.

[23] M. Sadeghi, F. Behnia and R. Amiri, "Optimal Sensor Placement for 2-D Range-Only Target Localization in Constrained Sensor Geometry," in IEEE Transactions on Signal Processing, vol. 68, pp. 2316-2327, 2020.

[24] W. Ji, X. Liu and E. Zou, "Range-free Localization Based on Adaptive Anchor Selection for Wireless Sensor Networks," 2019 IEEE/CIC International Conference on Communications in China (ICCC), 2019, pp. 775-779.

[25] H. Zhu, S. Chang, L. Lu and W. Zhang, "RUPS: Fixing Relative Distances among Urban Vehicles with Context-Aware Trajectories," 2016 IEEE International Parallel and Distributed Processing Symposium (IPDPS), Chicago, IL, USA, 2016, pp. 123-131

[26] H. Zhu, S. Chang, W. Zhang, F. Wu and L. Lu, "Online Vehicle Front–Rear Distance Estimation With Urban Context-Aware Trajectories," in IEEE Transactions on Vehicular Technology, vol. 67, no. 2, pp. 1063-1074, Feb. 2018.

[27] Y. Cai, H. Zhu, S. Chang, X. Wang, J. Shen and M. Guo, "PeerProbe: Estimating Vehicular Neighbor Distribution With Adaptive Compressive Sensing," in IEEE/ACM Transactions on Networking, vol. 30, no. 4, pp. 1703-1716, Aug. 2022.

[28] R. W. Tkach, "Network traffic and system capacity: Scaling for the future," 36th European Conference and Exhibition on Optical Communication, 2010, pp. 1-22.

[29] Haenggi M. Stochastic geometry for wireless networks[M]. Cambridge University Press, 2012.

[30] B. Mukhopadhyay, S. Srirangarajan and S. Kar, "RSS-Based Cooperative Localization and Edge Node Detection," in IEEE Transactions on Vehicular Technology, vol. 71, no. 5, pp. 5387-5403, May 2022.

Wengang Li received the B.Sc. and Ph.D. degrees in communication and information systems from Xidian University, Xi'an, China, in 2004 and 2010, respectively. He is currently an Associate Professor with the State Key Laboratory of Integrated Services Networks, Xidian University, and the School of Telecommunication Engineering, Xidian University. His research interests include navigation and positioning, broadband wireless communication, massive MIMO technology, satellite communications, and cognitive radio networks.

Mohan Liu received the bachelor's degree from China Jiliang University, Hangzhou, China, in 2021. He is currently a Master Student with the State Key Laboratory of Integrated Services Networks, Xidian University, and the School of Telecommunication Engineering, Xidian University. His research interests include navigation and positioning technology.

Tianfang Chen received the bachelor's degree from China University of Petroleum(East China), Qingdao, China, in 2021. He is currently a Master Student with the State Key Laboratory of Integrated Services Networks, Xidian University, and the School of Telecommunication Engineering, Xidian University. His research interests include navigation and positioning technology.

Guoqiang Mao received the B.Sc. and Ph.D. degrees in Telecommunications from Edith Cowan University, Australia, in 1999 and 2002, respectively. He is currently an Associate Professor with the State Key Laboratory of Integrated Services Networks, Xidian University, and the School of Telecommunication Engineering, Xidian University. His research interests include internet of vehicles, the internet of things, intelligent transport system, Wireless positioning technology .